J Mater Sci (2008) 43:4050–4056
DOI 10.1007/s10853-007-2225-2

REES RAWLINGS FESTSCHRIFT

Current-activated pressure-assisted sintering (CAPAS) and nanoindentation mapping of dual matrix composites

K. Morsi · V. V. Patel · K. S. Moon · J. E. Garay

Received: 15 June 2007 / Accepted: 11 October 2007 / Published online: 3 April 2008

Abstract Titanium boride (TiB_w) whiskers are currently recognized as one of the most compatible reinforcements for titanium (Ti) that have positively affected its wear resistance and stiffness. The fracture toughness and ductility have, however, been reported to deteriorate at increased TiB_w volume fractions, mainly due to the interlocking of these brittle TiB whiskers. This article investigates the processing of dual matrix Ti–TiB_w composites, where microstructures are generated consisting of TiB_w–Ti composite regions separated by a ductile, predominantly Ti, outer matrix. This microstructural design has the potential to prevent the continuous TiB_w interlocking over the scale of the composite (at high TiB_w volume fractions), and promote improved toughness of the material. The processing of these unique composites using current-activated pressure-assisted sintering (CAPAS) is discussed in this article. The effect of processing temperature on the microstructure and hardness of Ti–TiB_w dual matrix composites is also discussed, together with a simultaneous imaging and modulus-mapping nanoindentation technique used to characterize the composites

Introduction

The low stiffness and wear resistance of titanium (Ti) alloys have prompted researchers to consider composite strategies to overcome these deficiencies. The choice of a reinforcement for Ti is not a trivial matter, and out of many possible reinforcements, in situ-formed TiB whiskers have emerged as one of the most compatible and effective reinforcements for Ti [1]. This reinforcement is both chemically and mechanically compatible; however, the benefits of adding these reinforcements is not without a penalty. It has been recently reported that reductions in both fracture toughness and ductility are observed at TiB_w volume fractions where they interlock [2, 3]. The present authors believe that this shortcoming can be overcome by reinforcing the Ti with TiB_w only in localized regions within the microstructure, while always keeping a Ti phase in between these now composite regions. The result is a dual matrix microstructure (i.e., an inner Ti matrix 'within' the reinforced region, and an outer Ti matrix 'in between' the reinforced regions).

Work on dual matrix microstructural design has been reported for other material systems and reinforcement geometries including microstructurally toughened (MT) composites [4] where aluminum (Al) 6061 was reinforced with SiC_p-Al 6061 composite fibers. These produced composites with an order of magnitude higher impact toughness compared with conventional SiC-6061 composites. Also unique properties were recently reported for tungsten carbide (WC)–cobalt (Co) dual matrix composites, or double-cemented carbides [5, 6], with the intergranular mean free path being a governing parameter in controlling the properties. The present authors believe that titanium composites stand to benefit from this microstructural design, which could ultimately allow the tailorability of Ti–TiB_w composites, especially with the current problem of TiB_w interlocking at higher TiB_w volume fractions [7]. The processing steps used in previous work for other material systems have so far been generally considerable in

K. Morsi (✉) · V. V. Patel · K. S. Moon
Department of Mechanical Engineering, San Diego State University (SDSU), 5500 Campanile Drive, San Diego, CA, USA
e-mail: kmorsi@mail.sdsu.edu

J. E. Garay
Department of Mechanical Engineering, University of California, Riverside, CA, USA

number which would add to the cost of titanium composites. Our current work simplifies the number of processing steps. Powder processing and green compact design needs careful consideration in the case of Ti–TiB_w in situ dual matrix composites. Moreover, the in situ formation of TiB_w in localized regions also requires careful attention. The present article describes procedures for mechanically activating Ti–TiB_2 composite powder reinforcements in addition to electric current activation to promote rapid in situ transformation kinetics of Ti–TiB_2 composite powders to form TiB_w–Ti reinforcements in localized regions, during current-activated pressure-assisted sintering (CAPAS). Recent work by three of the authors [8] has largely focused on the use of different boron sources, ball milling, pressure-less sintering of dual matrix composites, and preliminary work on the use of current activation. It was determined that unlike pressure-less sintering, electric current activation can be successful in producing fully converted in situ TiB whiskers. The current work examines the effect of consolidation temperature during CAPAS on the microstructure and hardness of the processed dual matrix composites. Moreover, a simultaneous imaging and modulus-mapping technique was used to characterize the processed composites.

The CAPAS method

The CAPAS method is receiving worldwide attention due to its ability to efficiently consolidate powders into useable bulk materials [9]. For metals, this is achieved by passing high electric currents through powders in a die under an applied pressure. It should be noted that this method is often called spark plasma sintering (SPS) or pulsed electric current sintering (PECS). The term CAPAS is used here to emphasize the fact that it is the combined effects of high-density electric currents and pressure to which the method owes its success. The high current densities typical of the process should be effective in the present work which requires both densification and reaction of the initial powders. High current densities have been shown to significantly enhance intermetallic reaction rates [10, 11] independently of temperature. A possible mechanism for the increased kinetics is the lowering of the migration energy of point defects [12]. The applied pressure facilitates other densification mechanisms (besides sintering) such as creep, grain boundary sliding, and superplasticity.

Experimental procedures

Commercially pure Ti (−325 mesh) and TiB_2 (1–10 μm) powders (Atlantic Equipment Engineers, NJ, USA) were used as the starting powders. Powders were first rotator mixed for 30 min and vacuum degassed at 120 °C for 10 h before ball milling. A mixture of titanium and titanium diboride (34.14 wt.% TiB_2) powder were ball-milled using WC-Co balls for 5 h (interrupted runs) in a SPEX 8000 mixer under an argon atmosphere with a 15:1 ball-to-powder weight ratio. The application of ball milling here serves two purposes. The first is to embed the TiB_2 particles inside titanium powder, and the second is to generate crystallographic defects (i.e., mechanical activation) that would enhance high temperature diffusion kinetics during high temperature consolidation. Classified TiB_2−Ti ball-milled composite powders (63–90 μm) were then gently mixed for 30 min in a rotator mixer with an equal volume of Ti powder (un-milled), generating the dual matrix composite powder mix. The powders were then placed in a graphite die with an internal diameter of 19 mm, to generate a disc of this diameter and ∼2 mm thick. A pressure of 70 MPa was initially applied for 1 min to ensure the contacting of individual powders. After removing the pressure, a direct electric current (1000–1500 A) was applied for approximately 5 min without pressure. It was observed that the temperature of the die was raised nearly to the processing temperature within this period through joule heating. Then the load was gradually increased (10 kN/min) to 30 kN; at this load the nominal pressure on the sample was 106 MPa. The powders were then allowed to consolidate and react for an additional 17 min at a constant pressure of 106 MPa. Hence, the pressure was kept constant at 106 MPa for all experiments, and the processing temperature was investigated as the variable (1000, 1100, and 1200 °C). The temperature was measured using a thermocouple (Type N, Omega Engineering) placed in a hole positioned halfway through the external wall of the die directly inline with the sample. The temperature at this position is known to be less than 5 °C different from the sample temperature for widely ranging sample types [13]. Temperature in the CAPAS method comes exclusively from the high-density electric currents that pass through the sample/die system. The processing temperature quoted was controlled through a continuously varying current (between 1000 and 1500 A) during the experiment. The die was then allowed to cool down to room temperature. All CAPAS experiments were conducted under vacuum ($<4 \times 10^{-3}$ Torr).

A novel scanning technique was used to obtain an elastic modulus map of Ti–TiB_w dual composite surface with the resolution below the optical limit. Figure 1 shows the measurement principle of the forced scanning technique with a constant force. As can be seen from the figure, under a constant force of the probe tip, the stiff areas on the specimen allow less penetration of the tip than the soft areas. This variation of tip penetrations provides the

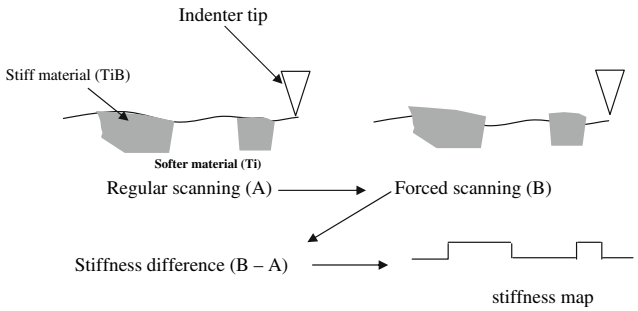

Fig. 1 Measurement principle of the forced scanning technique

relative stiffness information of the specimen surface. For the experimental setup, an SDSU-built nanoindentation system [5] with a Berkovich diamond indenter tip was used.

For microstructural examination, the specimens were cut, ground, and polished to 1-micron finish. Etching was performed in Kroll's reagent, and the microstructure was characterized using electron microscopy (secondary electron and backscattered, Hitachi S-2700). X-ray diffraction (XRD) (using Cu-K_{α}, Panalytical Xpert Pro diffractometer) was also used for phase analysis. Porosity was measured using image analysis of the polished samples. The macrohardness of the samples was measured with a Vickers hardness tester, using a 50 kg indentation load; care was exercised to ensure the indentation size covers the main microstructural features of our dual matrix composite. Five indents were made for each specimen and the average and standard deviation reported.

Results and discussion

X-ray diffraction of the ball-milled powders (reported by the authors elsewhere [8]) revealed significant peak broadening, signifying mechanical activation of the TiB_2–Ti precursor powders. Furthermore, current activation at CAPAS temperatures of 1100 °C was found to rapidly anneal these powders, such that XRD of processed composites revealed no retained peak broadening, unlike the pressure-less sintered counterpart. Figure 2a–c are low-magnification micrographs, showing the dual matrix microstructures of specimens processed using CAPAS at 1000, 1100, and 1200 °C, which contain dark TiB_w–Ti composite reinforcements surrounded by a predominantly Ti continuous outer matrix. It is clear that the microstructure contains a low level of porosity; image analysis has shown that the porosity levels for all processed specimens fall below 2%.

The outer Ti matrix is not free of whiskers, as can be seen from Fig. 3, some whiskers are also present (but at a

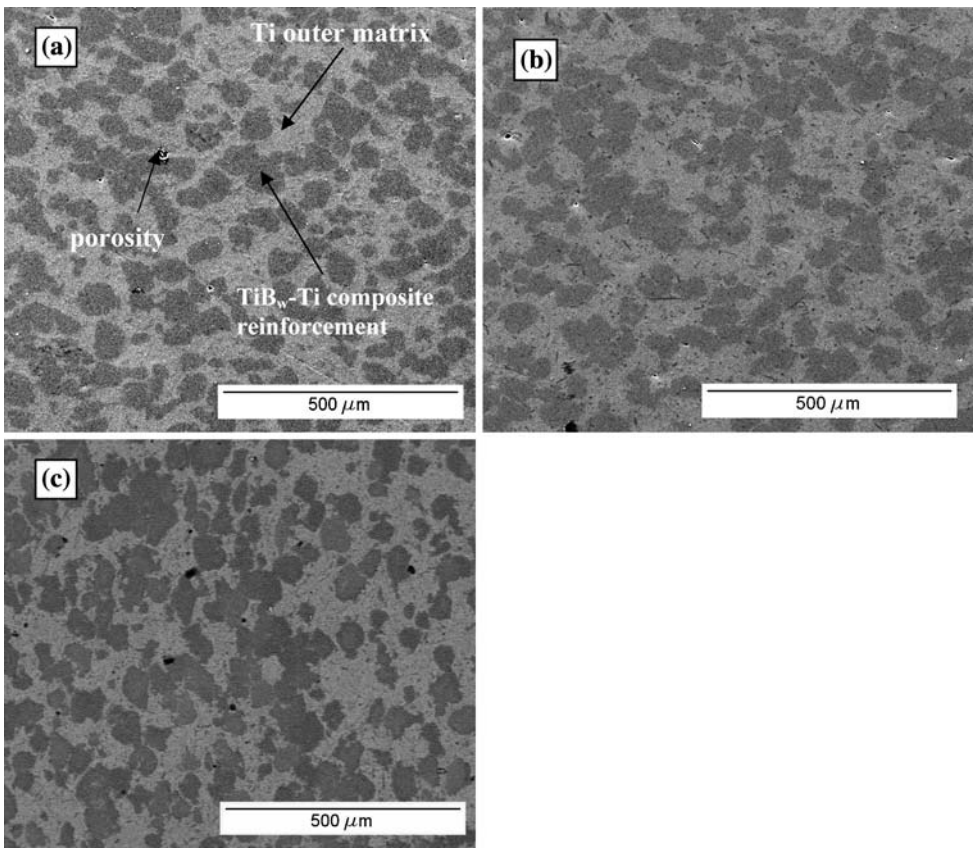

Fig. 2 SEM micrographs of dual matrix Ti–TiB_w composites produced by CAPAS at (**a**) 1000 °C, (**b**) 1100 °C, and (**c**) 1200 °C

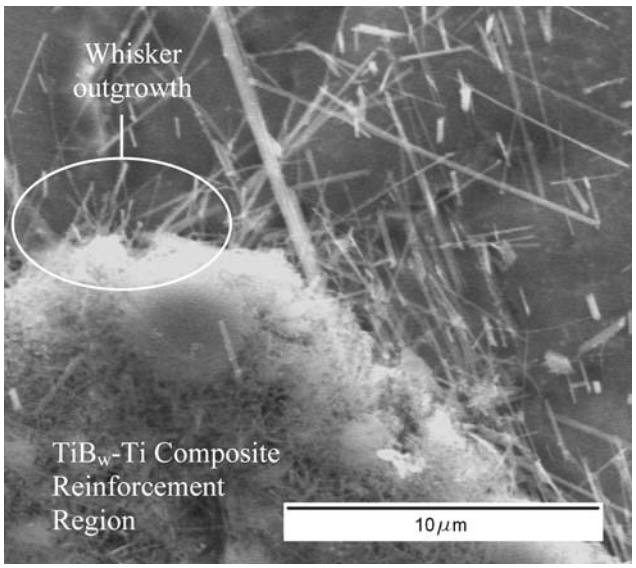

Fig. 3 High-magnification scanning electron micrograph of etched sample showing the interface between the TiB_w–Ti composite reinforcement region and Ti outer matrix, for a specimen processed at 1100 °C

much lower amount than TiB whiskers inside the composite reinforcements), especially closer to the TiB_w–Ti/Ti interface. We believe this maybe due to either outgrowth of TiB whiskers from the TiB_w-rich regions into the Ti outer matrix and possibly TiB_2 present at the surface of the ball-milled powders may have entered the Ti outer matrix powder during the rotator mixing stage, and transformed to TiB_w during processing. Figure 3 shows clear evidence of whisker outgrowth from the highly reinforced composite regions into the initially un-reinforced outer matrix Ti regions (note that the outer matrix Ti has been etched out, leaving outgrown whiskers behind). Other observed whiskers that are not emerging from the composite reinforcement shown in the image maybe extending out from other composite reinforcement(s) lying beneath the surface.

Figure 4a–c are high-magnification SEM micrographs of the composite reinforcement regions for specimens processed using CAPAS at 1000, 1100, and 1200 °C. Note the fine scale of the TiB whiskers being generated (largely submicron). Feng et al. [14], starting with elemental boron as the boron source, reported TiB whisker diameters of 0.5 μm when spark plasma sintering (SPS) was carried out at 1000 °C and 2 μm when 1200 °C was used. In another study, also by Feng et al. [15], similar findings where also reported when TiB_2 was used as the boron source.

It can be seen from Fig. 4a–c, that a high level of whisker interlocking is quite evident in these composite-reinforced regions (however that is not the case within the outer Ti matrix regions). Within the highly

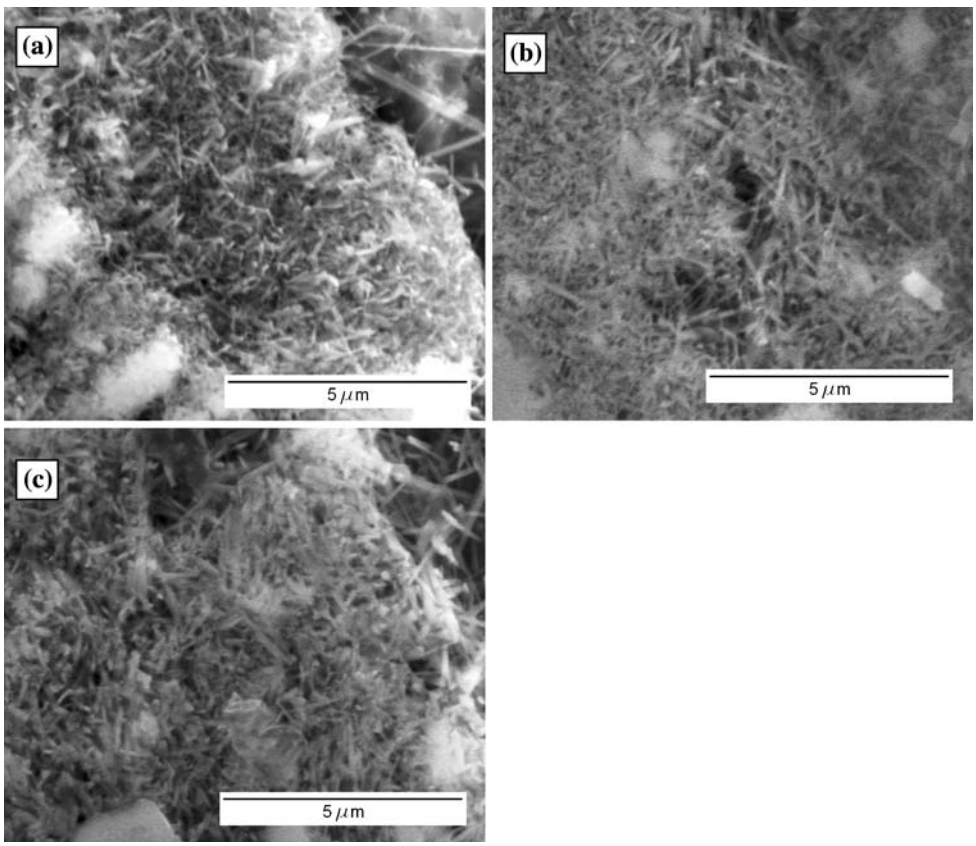

Fig. 4 High-magnification SEM images of the etched TiB_w–Ti composite-reinforced regions for specimens processed using CAPAS at (**a**) 1000 °C, (**b**) 1100 °C, and (**c**) 1200 °C

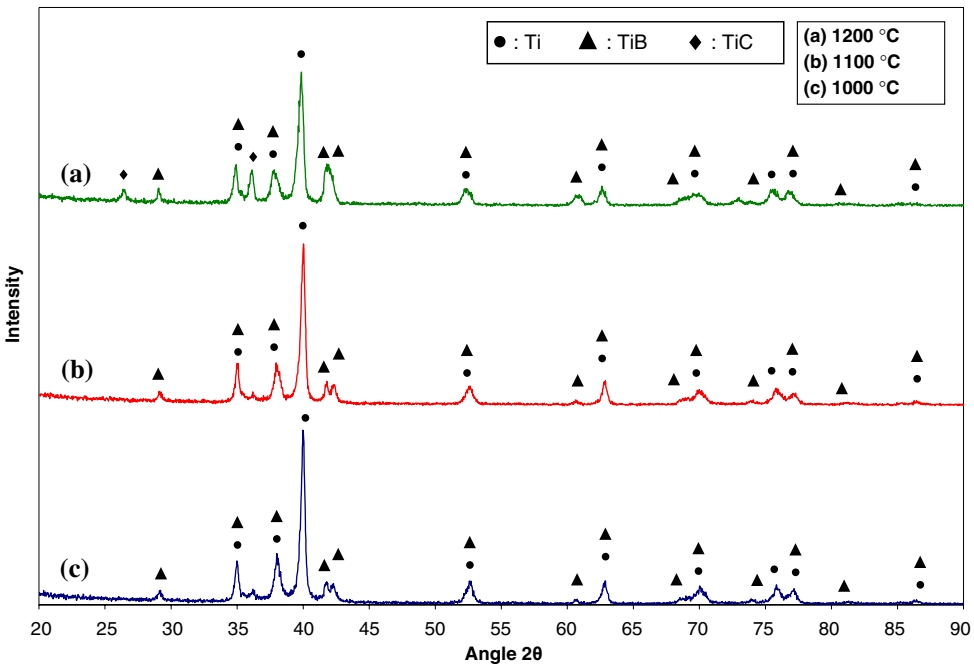

Fig. 5 XRD scans of specimens processed using CAPAS at 1000, 1100, and 1200 °C

TiB_w-reinforced regions, there exists light patches/regions; close examination of these regions reveals that they are highly agglomerated/clustered TiB_w. We can also see a general increase in whisker size with processing temperature, from 1000 to 1200 °C, this is in agreement with recent work where processing temperature has been reported to influence the TiB_w size [16].

Figure 5 is an XRD scans of the surfaces of materials processed at the three CAPAS temperatures investigated. It can be seen that at 1000 and 1100 °C the peaks predominantly belong to Ti and titanium boride (with a possible trace of titanium carbide (TiC)), with no residual TiB_2. This is also true for specimens processed at 1200 °C; however, in this case significant titanium carbide peaks are also observed. Using graphite as a die material in current-activated work, we believe it has resulted here in the diffusion of carbon to the specimen and subsequent reaction with Ti to form TiC at the 1200 °C processing temperature.

Vickers hardness measurements along the central cross-sectional line (perpendicular to the CAPAS pressing direction) of the processed materials are displayed in Fig. 6. Although the error bars are somewhat overlapping, there is a general increase in average hardness for the 1200 °C-processed materials (despite having coarser TiB_w). This, we believe, could be due to the noticeable formation of titanium carbide hard phase at this processing temperature (Fig. 5).

Elastic modulus map of Ti–TiB_w composites

The mechanical property measurement of a complex structure like Ti–TiB_w composites, that include very hard materials in the form of whiskers that can range from a few microns to nanometers in size, is very difficult even with recent nanoindentation systems that allow the imaging of surface features below the optical limit [17–19]. In a conventional nanoindentation experiment, mechanical properties are evaluated by using a rigid probe of well-defined shape to elastically or plastically deform a specimen, while monitoring the load and displacement response [20]. Furthermore, to construct a modulus map of the sample, thousands of indents have to be performed, which is very time consuming. Recently, a nanoindentation instrument, that is capable of measuring contact stiffness using force modulation technique, has been introduced [19] and various nanoindentation and modulus-mapping experiments have been conducted with the technique [21]. In this

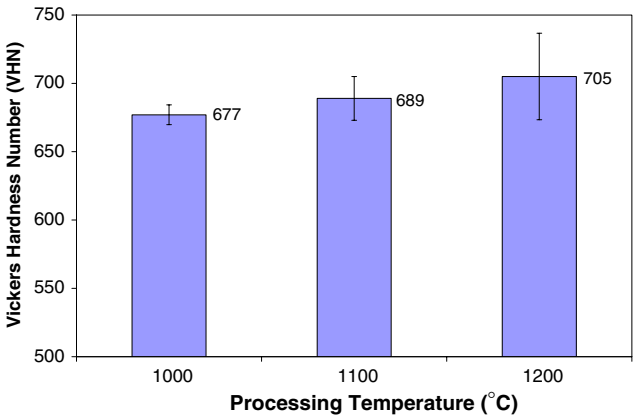

Fig. 6 Effect of CAPAS processing temperature on Vickers hardness number of processed materials

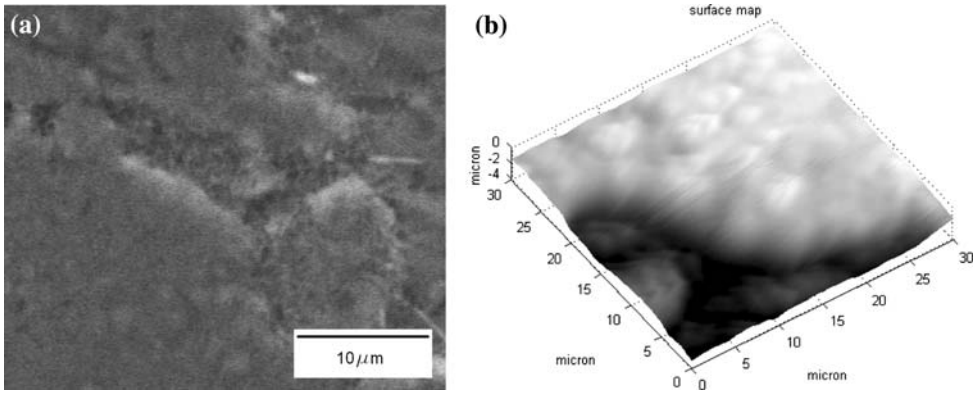

Fig. 7 (**a**) SEM micrograph of 1100 °C CAPAS specimen showing TiB_w-reinforced regions separated by predominantly un-reinforced regions and (**b**) Scanned image of the same sample produced using SDSU's nanoindentation system showing similar features

section, we present the experimental results of the modulus mapping of Ti–TiB_w dual matrix composites with a nanoindentation system developed at San Diego State University. This developed system is suitable for nanoindentation and modulus-mapping measurements for 'hard' materials such as Ti–TiB_w composites, as opposed to polymers.

Previous work [22] has shown that indentation tests conducted on etched Ti–TiB_w composite surfaces might produce undesired indentation results since etching in Kroll's reagent generates significant surface roughness on the composite surface. Therefore, well-polished surfaces give the best results.

Figure 7a, b are scanned images of the 1100 °C CAPAS specimen microstructure. They show similarity of the microstructural features observed using the SEM (Fig. 7a) and our nanoindentation system (Fig. 7b, pre-scanned under regular surface imaging mode), namely composite reinforcements next to predominantly un-reinforced Ti regions.

The same surface area of Fig. 7b was then scanned with the diamond tip at a constant contact force of 5.4 mN. During scanning, the indenter tip was modulated at a frequency of 165 Hz and with an oscillation displacement of 70 nm. The stiffness difference and the modulus value at each pixel point were calculated using the principle of Fig. 1 and the Hertzian dynamic model [23]. Figure 8a shows the obtained modulus map of the sample. As noted from Fig. 8b, the formation of TiB whisker clusters within the composite reinforcement is also evident in the modulus map. From the modulus map, the Young's modulus values of the peak TiB_w areas are distributed between 400 and 600 GPa, while the deep valley areas (Ti) yield the modulus values between 100 and 150 GPa. It should be mentioned that in our 1100 °C-processed material only a trace of TiC was detected by XRD which we believe will not significantly affect our results. The results are, however, consistent with previously published data [24], where the mean elastic modulus of aligned TiB whiskers in a Ti matrix parallel to the extrusion direction was reported to be

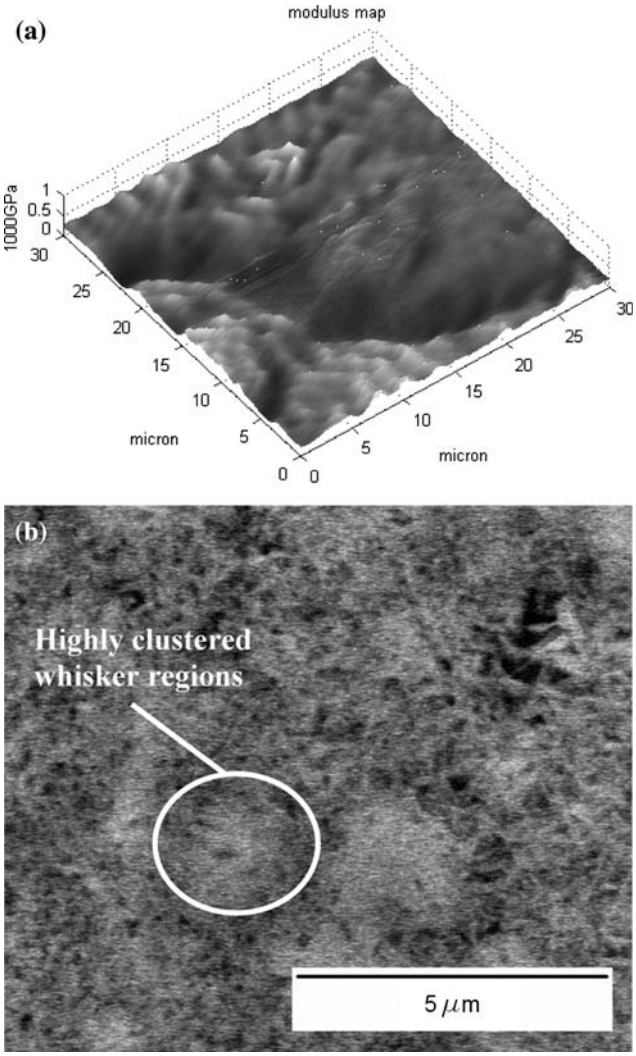

Fig. 8 (**a**) Modulus map of etched Ti–TiB_w composite sample of Fig. 7b (there is some noise in the image) and (**b**) High-magnification SEM micrograph showing clusters of TiB whiskers within the composite reinforcements

450 GPa (with a standard deviation of 45), while the mean TiB_w elastic modulus normal to the extrusion direction yielded a value of 514 GPa (with a standard deviation of

135). The authors, however, reported an average value of 482 GPa, considering both the results.

Although conventional Ti–TiB_w composites have been previously processed using current-activated methods [14, 15], the present work represents to the best of the authors' knowledge the first implementation of the dual matrix design to Ti–TiB_w composites, which should have significant implications for Ti composite development in general. For example, from previous work on other systems, it is reasonable to expect an increase in toughness and wear resistance for dual matrix Ti–TiB_w composites over conventional Ti–TiB_w composites. Our work has also shown that CAPAS can be successfully used to process these unique composites.

Conclusions

A powder processing sequence including ball milling was used to generate a precursor dual matrix powder mix that allowed the in situ generation of TiB_w whiskers in predominantly localized regions of the Ti microstructure during high temperature consolidation. CAPAS was used as the high-temperature powder consolidation method to successfully process high-density Ti–TiB_w dual matrix composites in short processing times. Increasing the CAPAS processing temperature was found to result in an increase in TiB whisker size, and the noticeable formation of TiC phase (in this case, at the highest processing temperature of 1200 °C) due to diffusion of carbon from the graphite die/plunger into the composite. The formation of TiC subsequently resulted in an increase in the Vickers hardness of composites processed at 1200 °C. A nanoindentation modulus-mapping technique was used to scan these unique microstructures and generate a modulus map of the phases.

Acknowledgements The authors would like to thank Dr. Steve Barlow for his help with electron microscopy, and Mr. Greg Morris and Mr. Michael Lester for their technical assistance throughout this project.

References

1. Gorsse S, Chaminade JP, Petitcorps YL (1998) Composites Part A 29(A):1229
2. Morsi K, Patel VV (2007) J Mater Sci 42:2037
3. Banerjee R, Collins PC, Fraser HL (2002) Adv Eng Mater 4(11):847
4. Nardone VC, Strife JR, Prewo KM (1991) Metal Mater Trans 22A:171
5. Deng X, Patterson BR, Chawla KK, Koopman MC, Fang Z, Lockwood G, Griffo A (2001) Int J Refractory Metals Hard Mater 19:547
6. Deng X, Patterson BR, Chawla KK, Koopman MC, Mackin C, Fang Z, Lockwood G, Griffo A (2002) J Mater Sci Lett 21:707
7. Fang Z, Lockwood G, Griffo A (1999) Metal Mater Trans 30A:3231
8. Morsi K, Patel VV, Naraghi S, Garay JE (2008) J Mater Process Technol 196(1):236
9. Munir ZA, Anselmi-Tamburini U, Ohyanagi M (2006) J Mater Sci 41:763
10. Anselmi-Tamburini U, Garay JE, Munir ZA (2005) Mater Sci Eng A 407:24
11. Garay JE, Anselmi-Tamburini U, Munir ZA (2003) Acta Mater 51:4487
12. Garay JE, Glade SC, Anselmi-Tamburini U, Asoka-Kumar P, Munir ZA (2004) Appl Phys Lett 85(4):573
13. Wang X, Casolco SR, Xu G, Garay JE (2007) Acta Mater 55:3611
14. Feng H, Zhou Y, Jia D, Meng Q (2004) Compos Sci Technol 64(16):2495
15. Feng H, Jia D, Zhou Y (2005) Composites: Part A 36:558
16. Panda KB, Ravi Chandran KS (2003) Metal Mater Trans 34A(6):1371
17. Stephen AJ, Houston JE (1991) Rev Sci Instrum 62(3):710
18. Pethica JB, Oliver WC (1987) Phys Scr T19A:61
19. Syed Asif SA, Wahl KJ, Colton RJ (1999) Rev Sci Instrum 70(5):2408
20. Oliver WC, Pharr GM (1992) J Mater Res 7(6):1564
21. Uskokovic PS, Tang CY, Tsui CP, Ignjatovic N, Uskokovic DP (2007) J Eur Ceram Soc 27(2–3):1559
22. Moon KS, Morsi K, Hong YK (2007) Int J Optomechatron 1:1
23. Chakravartula A, Komvopoulos K (2006) Appl Phys Lett 88:131901
24. Gorsse S, Miracle DB (2003) Acta Mater 51:2427